



## Comparative structural coordination chemistry of two tricyclic bisamidines

Jingwei Li<sup>a</sup>, Daniel W. Widlicka<sup>a</sup>, Kerry Fichter<sup>a</sup>, David P. Reed<sup>a</sup>, Gary R. Weisman<sup>a,\*</sup>, Edward H. Wong<sup>a,\*\*</sup>, Antonio DiPasquale<sup>b</sup>, Katie J. Heroux<sup>b</sup>, James A. Golen<sup>c</sup>, Arnold L. Rheingold<sup>b</sup>

<sup>a</sup> Department of Chemistry, University of New Hampshire, Durham, NH 03824, USA

<sup>b</sup> Department of Chemistry and Biochemistry, University of California, San Diego, La Jolla, CA 92093, USA

<sup>c</sup> Department of Chemistry and Biochemistry, University of Massachusetts Dartmouth, North Dartmouth, MA 02747, USA

### ARTICLE INFO

#### Article history:

Available online 13 August 2010

Dedicated to Professor Arnold L. Rheingold on the occasion of his 70th birthday.

#### Keywords:

Tricyclic bisamidine  
Metal complexes  
Crystal structures

### ABSTRACT

The tricyclic bisamidines **L1** and **L2** are designed to be prestrained so as to present synperiplanar donor sites for metal coordination. Their very different bite angles of 35° and 70° result from the incorporation of two five-membered instead of six-membered rings in their respective backbones. Distinct coordination preferences in a variety of metal complexes have now been confirmed by X-ray structural studies. While **L1** afforded monodentate, symmetrical and unsymmetrical chelating as well as bimetallic bridging modes in its complexes, **L2** has been found exclusively in a bidentate chelating mode.

© 2010 Elsevier B.V. All rights reserved.

## 1. Introduction

Unsaturated bidentate nitrogen-based ligands are important chelators in metal coordination chemistry providing many complexes of interest for their catalytic, bioinorganic, photochemical, and photophysical applications. These are epitomized by 2,2-bipyridyl [1–4] and related ligands like phenanthroline [5,6], biimidazole [7,8] and bioxazolines [9–11]. We have reported a bisamidine **L1** with synperiplanar donor sites enforced by its tricyclic backbone constraints. Due to its relatively small idealized bite angle of 35° [12–14], it has been found to adopt monodentate, symmetrical and unsymmetrical chelating as well as bridging coordination modes in its metal complexes (Fig. 1) [12]. We now describe new Pd(II), Zn(II), Ag(I), and Hg(II) complexes of this ligand whose structures further confirm this versatility in metal binding. Since the tricyclic nature of **L1** allows significant tuning of its ideal bite angle through variations in ring sizes, we have prepared a new bisamidine, **L2**, featuring three six-membered rings in its backbone (Fig. 1) whose lone pairs are expected to be considerably more convergent (idealized bite angle 70°) [14]. We have prepared and determined structures of five of these metal complexes to confirm its predilection for the chelation coordination mode.

## 2. Experimental

### 2.1. General

Bisamidine **L1** was prepared as described by Reed and Weisman [15]. *N,N'*-bis-(3-aminopropyl)-1,2-ethylenediamine was purchased from Sigma–Aldrich Chemical Co. Dithiooxamide was obtained from Fluka Chemical Co. All other reagents and solvents were also obtained from commercial sources and used without further purification. Deuterated solvents were obtained from Cambridge Isotope Laboratories and stored over 3 Å molecular sieves.

All <sup>1</sup>H and <sup>13</sup>C{<sup>1</sup>H} NMR spectra were acquired on either a Varian Mercury 400 MHz spectrometer operating at 399.75 and 100.51 MHz respectively or on a Varian Unity/NOVA 500 MHz spectrometer operating at 500 and 125.67 MHz respectively. IR spectra were recorded using KBr pellets on a Nicolet MX-1 FT spectrophotometer. ESI-MS was performed on a Thermofinnigan LCQ Mass Spectrometer coupled to a Picoview electrospray source. FAB-MS was performed on the JEOL JMS-AX505HA Mass Spectrometer at the University of Notre Dame. Electronic spectra were measured using a Cary 219 spectrophotometer. Elemental analysis was performed at Atlantic Microlab Inc., Norcross, GA.

All reactions were performed in standard Schlenk glassware under a nitrogen atmosphere. Recrystallizations were conducted in closed containers without special precautions to exclude either air or moisture. Bulk solvent removal was by rotary evaporation under reduced pressure and trace solvent removal from solids was by vacuum pump evacuation.

\* Corresponding author. Tel.: +1 603 862 1550; fax: +1 603 862 4278.

\*\* Corresponding author. Tel.: +1 603 862 1550; fax: +1 603 862 4278.

E-mail addresses: [gary.weisman@unh.edu](mailto:gary.weisman@unh.edu) (G.R. Weisman), [ehw@cisunix.unh.edu](mailto:ehw@cisunix.unh.edu) (E.H. Wong).

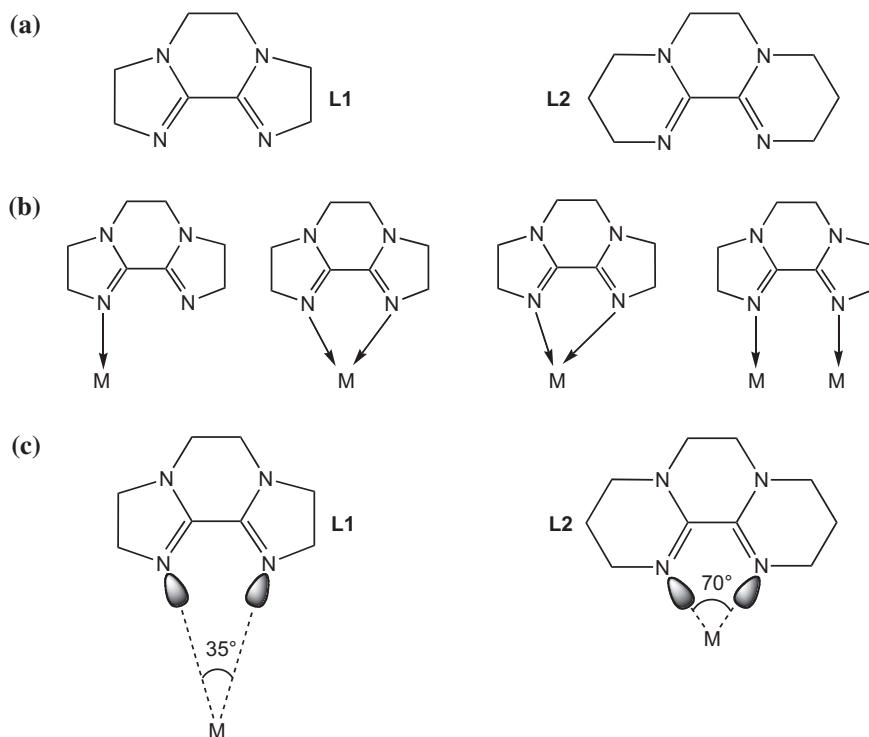


Fig. 1. (a) Tricyclic bisamidine **L1** and **L2**; (b) **L1** coordination modes; and (c) Ideal bite angles for **L1** and **L2**.

Idealized bite angles for ligands **L1** and **L2** were calculated using the molecular mechanics program MM2 in CHEM3D.

Caution! Perchlorate salts of metal complexes containing organic ligands in organic solvents are potentially explosive. Although no problems were encountered by us, cautious handling of only small amounts of these compounds should be the rule.

## 2.2. Experimental

### 2.2.1. 2,3,4,6,7,9,10,11-Octahydro-pyrazino[1,2-a:4,3-a']dipyrimidine (**L2**)

A 250 mL three-necked round-bottomed flask equipped with a reflux condenser with N<sub>2</sub> inlet tube, a fritted gas dispersion tube (initially closed) and a pressure-equalizing addition funnel was charged with dithiooxamide (2.00 g, 16.6 mmol) suspended in absolute EtOH (30 mL). A solution of *N,N'*-bis-(3-aminopropyl)-1,2-ethylenediamine (2.90 g, 16.6 mmol) in absolute EtOH (20 mL) was added by syringe. The nitrogen manifold exit line was routed through two scrubbing towers charged with 30% aqueous NaOH solution in order to trap the gases evolved. The reaction mixture was heated at 80 °C for 2 h. The reaction mixture was then cooled to room temperature and EtOH (30 mL) was added in order to immerse the fritted gas dispersion tube. Residual gaseous byproducts were purged from the solution by entrainment with nitrogen for 24 h. Solvent was then removed by rotary evaporation leaving a thick dark-red liquid, which was dissolved in CHCl<sub>3</sub> (100 mL) and filtered through glass wool. CHCl<sub>3</sub> was removed by rotary evaporation and toluene (100 mL) was added followed by heating. The near-boiling mixture was filtered through glass wool. The toluene extracts were azeotropically distilled over a Dean-Stark trap for 2 days. Evaporation of the resulting bright dark-yellow solution under reduced pressure afforded a yellow solid (1.74 g, 55% yield). <sup>1</sup>H NMR (CDCl<sub>3</sub>, 399.75 MHz): δ 1.85 (~p, 4H, *J*<sub>app</sub> = ~6 Hz, N-CH<sub>2</sub>-CH<sub>2</sub>-CH<sub>2</sub>-N=), 3.21 (~t, 4H, *J*<sub>app</sub> = ~6 Hz, N-CH<sub>2</sub>-CH<sub>2</sub>-CH<sub>2</sub>-N=), 3.22 (s, 4H, N-CH<sub>2</sub>-CH<sub>2</sub>-N), 3.54 (~t, 4H, *J*<sub>app</sub> = ~6 Hz, N-CH<sub>2</sub>-CH<sub>2</sub>-CH<sub>2</sub>-N=); <sup>13</sup>C{<sup>1</sup>H} NMR (CDCl<sub>3</sub>,

100.51 MHz, ref. center line of CDCl<sub>3</sub> set at 77.3 ppm) δ 21.52, 45.00, 47.66, 48.06, 148.04; <sup>1</sup>H NMR (CD<sub>3</sub>CN, 399.75 MHz): δ 1.73–1.78 (m, 4H), 3.18–3.20 (m, 4H), 3.18 (s, 4H), 3.35 (~t, 4H); <sup>13</sup>C{<sup>1</sup>H} NMR (CD<sub>3</sub>CN, 100.51 MHz, ref. center line of CD<sub>3</sub>CN set at 117.62) δ 21.53, 44.38, 47.45, 47.63, 148.03; IR (KBr): 1601 cm<sup>-1</sup> (N=C-C=N); UV-Vis (CH<sub>3</sub>CN): 248 nm (ε = 7500 M<sup>-1</sup> cm<sup>-1</sup>); Anal. Calc. for C<sub>10</sub>H<sub>16</sub>N<sub>4</sub>·(H<sub>2</sub>O)<sub>0.8</sub>: C, 58.12; H, 8.58; N, 27.11. Found: C, 58.18; H, 8.66; N, 26.79%. (This material was of sufficient purity for metal complexations. Purification by sublimation twice (130 °C/~20 Torr) afforded a lighter yellow product. Recrystallization from hexane or heptane followed by sublimation gave a pure white product.)

A crude mixture obtained prior to the use of the toluene azeotropic distillation procedure was shown by NMR and MS analysis to be a mixture of **L2** and **A**. Spectra for **A**: <sup>1</sup>H NMR (CDCl<sub>3</sub>, 360.15 MHz, TMS): δ 1.8 (br, s, 2H, NH<sub>2</sub>), 1.72 (m, 2H, NCH<sub>2</sub>CH<sub>2</sub>CH<sub>2</sub>N=, *J* = 6.7 Hz), 1.85 (p, 2H, NCH<sub>2</sub>CH<sub>2</sub>CH<sub>2</sub>NH<sub>2</sub>), 2.72 (t, 2H, CH<sub>2</sub>NH<sub>2</sub>, *J* = 6.6 Hz), 3.21–3.28 (m, 2H), 3.47–3.60 (m, 8H). <sup>13</sup>C{<sup>1</sup>H} NMR (CDCl<sub>3</sub>, 90.56 MHz, ref. central line of CDCl<sub>3</sub> at δ 77.23) δ 21.23 (NCH<sub>2</sub>CH<sub>2</sub>CH<sub>2</sub>N=), 30.79 (NCH<sub>2</sub>CH<sub>2</sub>CH<sub>2</sub>NH<sub>2</sub>), 39.05, 45.06, 45.10, 45.16, 46.92, 47.44, 147.80, 152.72. MS (EI): *m/z* 211.3 (M+1).

### 2.2.2. 1,4-Bis-(3-aminopropyl)-2,3-piperazinedione (**B**)

A crude mixture of **L2** and **A** was dissolved in D<sub>2</sub>O. NMR analysis was consistent with the formation of **B**. <sup>1</sup>H NMR (D<sub>2</sub>O, 360.15 MHz, ref. CH<sub>3</sub>CN set at 2.05 ppm) δ 1.74 (p, 4H), 2.62 (t, 4H), 3.49 (t), 3.65 (s, 4H); <sup>13</sup>C{<sup>1</sup>H} NMR (D<sub>2</sub>O, 90.56 MHz, ref. center peak of CH<sub>3</sub>CN set at 1.7 ppm) δ 29.85, 38.65, 44.83, 46.04, 159.20. This NMR sample was concentrated by rotary evaporation. EtOH (2 mL) was added the sample was again rotary evaporated to ensure the removal of residual D<sub>2</sub>O. NMR of this sample in CDCl<sub>3</sub> was consistent with a mixture of **A** and **B**, indicating partial dehydration.

### 2.2.3. 1,4-Bis-(2-aminoethyl)-2,3-piperazinedione (**C**)

**L1** was dissolved in H<sub>2</sub>O and left for 14 h. The solution was concentrated by rotary evaporation, the residue was dissolved in

CHCl<sub>3</sub>, and the solution was dried over Na<sub>2</sub>SO<sub>4</sub>. Concentration of the filtrate after the removal of the drying agent afforded a white waxy solid: m.p.: 111–112 °C; <sup>1</sup>H NMR (CDCl<sub>3</sub>, 360.15 MHz) δ 1.27 (br s, 4H, NH<sub>2</sub>), 2.95 (t, 4H, *J* = 6.3 Hz, CH<sub>2</sub>CH<sub>2</sub>NH<sub>2</sub>), 3.54 (t, 4H, *J* = 6.3 Hz, CH<sub>2</sub>CH<sub>2</sub>NH<sub>2</sub>), 3.64 (s, 4H, NCH<sub>2</sub>CH<sub>2</sub>N); <sup>13</sup>C NMR (CDCl<sub>3</sub>, 90.56 MHz, ref. central line of CDCl<sub>3</sub> set at 77.23 ppm) δ 39.92, 45.60, 50.76, 158.02; IR (KBr) 3387.7 (NH asym.), 3317 (NH sym.), 1667 cm<sup>-1</sup>; MS (CI, isobutane) *m/z* 183.2 (M-18+1) [16].

#### 2.2.4. [Pd(L2)<sub>2</sub>](BF<sub>4</sub>)<sub>2</sub>, complex 1

An amount of Pd(CH<sub>3</sub>CN)<sub>4</sub>(BF<sub>4</sub>)<sub>2</sub> (250 mg, 0.563 mmol) was dissolved in CH<sub>3</sub>CN (5 mL). Addition of 4.4 mL (222 mg, 0.5 mmol) CH<sub>3</sub>CN of this solution by syringe to **L2** (194 mg, 1.01 mmol) in a flask resulted in a yellow solution. The reaction mixture was stirred at room-temperature for 4 h. The solution was then transferred to test tubes for crystallization by slow Et<sub>2</sub>O diffusion. Yellow needles (236 mg, 71% yield) of complex **1** were harvested. <sup>1</sup>H NMR (CD<sub>3</sub>CN, 399.75 MHz): δ 1.95 (m, 4H), 3.39 (t, 4H), 3.40 (t, 4H), 3.45 (s, 4H); <sup>13</sup>C{<sup>1</sup>H} NMR (CD<sub>3</sub>CN, 100.51 MHz, ref. CD<sub>3</sub>CN set at 117.6 ppm): δ 20.1, 46.3, 46.8, 48.7, 155.0; IR (KBr): 1612 cm<sup>-1</sup> (N=C=C=N); ESI-MS: 557.1 amu [[Pd(L2)<sub>2</sub>](BF<sub>4</sub>)<sub>2</sub>]<sup>+</sup>; Anal. Calc. for Pd(C<sub>10</sub>H<sub>16</sub>N<sub>4</sub>)<sub>2</sub>(BF<sub>4</sub>)<sub>2</sub>·(H<sub>2</sub>O)<sub>1.5</sub>: C, 34.74; H, 5.10; N, 16.20. Found: C, 34.78; H, 4.84; N, 16.30%.

#### 2.2.5. [Pd<sub>2</sub>(L1)<sub>4</sub>]Br<sub>4</sub>, complex 2

An amount of Pd(PhCN)<sub>2</sub>Br<sub>2</sub> (114 mg, 0.241 mmol) and 2.20 equivalents of **L1** (90.8 mg, 0.533 mmol) were dissolved in 7 mL DMSO to give an orange solution. After stirring for 30 min, diethyl ether was slowly diffused in to give a yellow solid (134 mg, 23% yield). <sup>1</sup>H NMR (CD<sub>3</sub>OD, 499.775 MHz): δ 3.66 (s, 4H), 3.89–3.94 (AA'XX', 4H), 4.19–4.24 (AA'XX', 4H); <sup>13</sup>C{<sup>1</sup>H} NMR (CD<sub>3</sub>OD, 125.67 MHz, ref. CD<sub>3</sub>CN set at 117.6 ppm): δ 42.52, 49.47, 54.47, 153.63; IR (KBr): 1605, 1533 cm<sup>-1</sup> (N=C=C=N); UV-Vis (DMSO): 315 nm (ε = 50,200 M<sup>-1</sup> cm<sup>-1</sup>); ESI-MS: 1106.5 amu [[Pd<sub>2</sub>(L1)<sub>4</sub>]Br<sub>3</sub>]<sup>+</sup>; Anal. Calc. for Pd<sub>2</sub>(C<sub>8</sub>H<sub>12</sub>N<sub>4</sub>)<sub>2</sub>Br<sub>4</sub>·(H<sub>2</sub>O)<sub>4</sub>: C, 30.47; H, 4.48; N, 17.77; Br, 25.34. Found: C, 30.05; H, 4.55; N, 17.71; Br, 24.99%.

#### 2.2.6. Zn(L1)<sub>3</sub>(NO<sub>3</sub>)<sub>2</sub>, complex 3

An amount of Zn(NO<sub>3</sub>)<sub>2</sub>·6H<sub>2</sub>O (34.1 mg, 0.114 mmol) and a slight excess of three equivalents of **L1** (59.0 mg, 0.360 mmol) were dissolved in acetonitrile (5 mL) with stirring. The clear solution was subjected to ether diffusion. Clear rhombic crystals (54.6 mg, 0.0801 mmol, 70%) of **3** grew after 3 days. <sup>1</sup>H NMR (CD<sub>3</sub>CN): δ 3.41 (s, 4H), 3.55–3.73 (AA'XX', 4H), 3.75–3.93 (AA'XX', 4H); <sup>13</sup>C{<sup>1</sup>H} NMR (CD<sub>3</sub>CN, ref. CD<sub>3</sub>CN set at 117.6 ppm): δ 44.93, 53.02, 53.61, 156.64; IR (KBr): 1641, 1628, 1582, 1547 cm<sup>-1</sup> (N=C=C=N); Anal. Calc. for Zn(C<sub>8</sub>H<sub>12</sub>N<sub>4</sub>)<sub>3</sub>(NO<sub>3</sub>)<sub>2</sub>: C, 42.27; H, 5.32; N, 28.75. Found: C, 42.09; H, 5.37; N, 28.97%.

#### 2.2.7. Zn(L2)<sub>3</sub>(ClO<sub>4</sub>)<sub>2</sub>, complex 4

Addition of an amount of Zn(ClO<sub>4</sub>)<sub>2</sub>·6H<sub>2</sub>O (38.6 mg, 0.104 mmol) to a solution of **L2** (61.2 mg, 0.318 mmol) in CH<sub>3</sub>CN (20 mL) formed a colorless solution. After stirring for 2 h, this solution was transferred to vials for crystallization by diethyl ether diffusion. X-ray quality colorless crystals of **4** were harvested over several days (44 mg, 50% yield). <sup>1</sup>H NMR (CD<sub>3</sub>CN, 399.75 MHz): δ 1.70–1.85 (2m, 3 × 4H), 3.02–3.60 (m, 3 × 12H); <sup>13</sup>C{<sup>1</sup>H} NMR (CD<sub>3</sub>CN, 100.53 MHz, ref. CD<sub>3</sub>CN set at 117.7 ppm) δ 20.4, 42.5, 46.6, 47.3, 147.3; IR (KBr): 1614 cm<sup>-1</sup> (N=C=C=N); Anal. Calc. for Zn(C<sub>10</sub>H<sub>16</sub>N<sub>4</sub>)<sub>3</sub>(ClO<sub>4</sub>)<sub>2</sub>: C, 42.84; H, 5.75; N, 19.78; Cl, 8.43. Found: C, 42.61; H, 5.81; N, 19.71; Cl, 8.64%.

#### 2.2.8. [Hg(L2)<sub>2</sub>](HgCl<sub>4</sub>), complex 5

Addition of an amount of HgCl<sub>2</sub> (95.3 mg, 0.351 mmol) to a solution of **L2** (71.1 mg, 0.370 mmol) in MeOH (15 mL) resulted

in the precipitation of a white solid. After filtration, the product was washed with additional MeOH and dried under reduced pressure to give a white powder. Clear, colorless cubic crystals were harvested after Et<sub>2</sub>O diffusion into a DMF solution of this powder over several days (112 mg, 65% yield). <sup>1</sup>H NMR (CD<sub>3</sub>CN, 399.75 MHz): δ 1.93 (m, 4H), 3.37 (t, 4H), 3.42 (s, 4H), 3.51 (t, 4H); <sup>13</sup>C{<sup>1</sup>H} NMR (CD<sub>3</sub>CN, 100.52 MHz, ref. CD<sub>3</sub>CN set at 117.6 ppm) δ 20.1, 44.9, 46.6, 47.4, 148.0; MS (EI): 429.3 amu [[Hg(L2)Cl]<sup>+</sup>]; IR (KBr): 1608 cm<sup>-1</sup> (N=C=C=N); Anal. Calc. for Hg(C<sub>10</sub>H<sub>16</sub>N<sub>4</sub>)Cl<sub>2</sub>: C, 25.90; H, 3.48; N, 12.08; Cl, 15.29. Found: C, 25.99; H, 3.50; N, 11.93; Cl, 15.10%.

#### 2.2.9. [Hg(L1)Cl<sub>2</sub>]<sub>2</sub>, complex 6

An amount of HgCl<sub>2</sub> (38.4 mg, 0.103 mmol) was dissolved in 5 mL methanol. Upon addition of a methanol solution of **L1** (84.5 mg, 0.515 mmol in 5 mL) a white precipitate formed. After filtration, this solid was washed with methanol and dried under reduced pressure to give product as a white powder (34.5 mg, 86% yield). This was recrystallized from DMSO by ether diffusion to give clear cubic crystals. <sup>1</sup>H NMR ((CD<sub>3</sub>)<sub>2</sub>SO): δ 3.73–3.80 (AA'XX', 4H), 3.55–3.70 (AA'XX', 4H), 3.41 (s, 4H); <sup>13</sup>C{<sup>1</sup>H} NMR ((CD<sub>3</sub>)<sub>2</sub>SO, ref. center line of (CD<sub>3</sub>)<sub>2</sub>SO set at 39.51 ppm) δ 43.4, 51.7, 52.7, 154.7; IR (KBr): 1624, 1543 cm<sup>-1</sup> (N=C=C=N); Anal. Calc. for Hg(C<sub>8</sub>H<sub>12</sub>N<sub>4</sub>)Cl<sub>2</sub>: C, 22.05; H, 2.78; N, 12.86. Found: C, 22.22; H, 2.72; N, 12.67%.

#### 2.2.10. [Cu(L2)<sub>3</sub>](ClO<sub>4</sub>)<sub>2</sub>, complex 7

Addition of an amount of Cu(ClO<sub>4</sub>)<sub>2</sub>·(H<sub>2</sub>O)<sub>6</sub> (37.2 mg, 0.101 mmol) to a solution of **L2** (58.3 mg, 0.303 mmol) in MeCN (5 mL) resulted in the formation of a light blue solution. After stirring for 1 h, the solution was transferred to small vials for crystallization by diethyl ether diffusion. Clear, green X-ray quality crystals were harvested after several days. A total mass of 51.0 mg (60% yield) of the crystals were collected. IR (KBr pellet): 1615 cm<sup>-1</sup> (N=C=C=N); Anal. Calc. for Cu(C<sub>10</sub>H<sub>16</sub>N<sub>4</sub>)<sub>3</sub>(ClO<sub>4</sub>)<sub>2</sub>·(H<sub>2</sub>O): C, 42.03; H, 5.88; N, 19.61; Cl, 8.27. Found: C, 42.05; H, 5.83; N, 19.35; Cl, 8.18%.

#### 2.2.11. [Cu(L2)<sub>2</sub>](ClO<sub>4</sub>)<sub>2</sub>, complex 8

An amount of Cu(ClO<sub>4</sub>)<sub>2</sub>·(H<sub>2</sub>O)<sub>6</sub> (58.2 mg, 0.157 mmol) and two equivalents of **L2** (59.6 mg, 0.310 mmol) were combined in a flask. A blue precipitate formed immediately when EtOH (5 mL) was added into the flask. The product was collected by filtration and washed with additional MeOH, dried under reduced pressure to give a blue powder (65.7 mg, 66% yield). Clear, dark blue needle crystals were harvested after Et<sub>2</sub>O diffusion into a CH<sub>3</sub>CN solution of this powder over several days. IR (KBr): 1623 cm<sup>-1</sup> (N=C=C=N); Anal. Calc. for Cu(C<sub>10</sub>H<sub>16</sub>N<sub>4</sub>)<sub>2</sub>(ClO<sub>4</sub>)<sub>2</sub>: C, 37.13; H, 4.99; N, 17.32; Cl, 10.96. Found: C, 37.61; H, 5.00; N, 17.45%.

#### 2.2.12. [Ag(L2)<sub>2</sub>](BF<sub>4</sub>), complex 9

Addition of AgBF<sub>4</sub> (28.9 mg, 0.148 mmol) to a solution of **L2** (62.1 mg, 0.323 mmol) in MeCN (6 mL) generated a light yellow solution. This MeCN solution was transferred to test tubes for recrystallization by ether diffusion. Light yellow crystals (38.9 mg, 45% yield) were harvested from the solution after several days in the dark. <sup>1</sup>H NMR (CD<sub>3</sub>CN, 399.75 MHz, ref. center line of CD<sub>2</sub>H<sub>2</sub>CN set at 1.96 ppm): δ 1.85 (m, 4H), 3.30 (t, 4H), 3.32 (s, 4H), 3.46 (t, 4H); <sup>13</sup>C{<sup>1</sup>H} NMR (CD<sub>3</sub>CN, 100.52 MHz, ref. CD<sub>3</sub>CN set at 117.6 ppm) δ 20.7, 46.95, 46.98, 47.6, 148.4; IR (KBr): 1626, 1596 cm<sup>-1</sup> (N=C=C=N); Anal. Calc. for Ag(C<sub>10</sub>H<sub>16</sub>N<sub>4</sub>)<sub>2</sub>(BF<sub>4</sub>): C, 41.47; H, 5.57; N, 19.35. Found: C, 41.58; H, 5.64; N, 19.28%.

#### 2.2.13. [Ag(L2)<sub>2</sub>](BPh<sub>4</sub>), complex 10

Addition of a solution of AgBF<sub>4</sub> (48.8 mg, 0.251 mmol) in EtOH (2 mL) to a solution of **L2** (99.2 mg, 0.516 mmol) in EtOH (3 mL)

produced a cloudy light yellow solution. After stirring for 3 h in the dark, a solution of NaBPh<sub>4</sub> (88.1 mg, 0.257 mmol) in EtOH was added to exchange the counter anion BF<sub>4</sub><sup>-</sup>. Immediately, a white precipitate was formed. The white precipitate was filtered off and washed with additional EtOH, followed by drying under vacuum in the dark to give a white powder (144 mg, 71% yield). Clear,

colorless cubic crystals were harvested after Et<sub>2</sub>O diffusion into a DMF solution of this white powder in the dark over several days. <sup>1</sup>H NMR (CD<sub>3</sub>)<sub>2</sub>SO, 399.75 MHz): δ 1.75 (m, 4H), 3.25 (t, 4H), 3.29 (s, 4H), 3.37 (t, 4H), 6.78 (t, 4H), 6.92 (s, 4H), 7.17 (m, 4H); <sup>13</sup>C{<sup>1</sup>H} NMR ((CD<sub>3</sub>)<sub>2</sub>SO, 100.52 MHz, ref. center line of (CD<sub>3</sub>)<sub>2</sub>SO set at 40.2 ppm) δ 20.8, 46.7, 47.0, 47.6, 122.3, 126.0, 136.0,

**Table 1**

Crystal data for the new metal complexes of **L1** and **L2**. For full details, see the Supplementary material.

	Pd <sub>2</sub> L <sub>1</sub> Br <sub>4</sub> ( <b>2</b> )	ZnL <sub>1</sub> <sub>3</sub> (NO <sub>3</sub> ) <sub>2</sub> ( <b>3</b> )	ZnL <sub>2</sub> <sub>3</sub> (ClO <sub>4</sub> ) <sub>2</sub> ( <b>4</b> )
Chemical formula	C <sub>36</sub> H <sub>54</sub> Br <sub>4</sub> N <sub>18</sub> Pd <sub>2</sub>	C <sub>24</sub> H <sub>36</sub> N <sub>14</sub> O <sub>6</sub> Zn	C <sub>30</sub> H <sub>48</sub> C <sub>12</sub> N <sub>12</sub> O <sub>8</sub> Zn
Molecular weight	1271.41	682.04	841.07
Space group	<i>P</i> 2(1)/ <i>n</i>	<i>Pbcn</i>	<i>P</i> 2(1)/ <i>n</i>
Color	yellow	colorless	colorless
<i>a</i> (Å)	11.7786(7)	17.5946(8)	9.7049(7)
<i>b</i> (Å)	17.2310(10)	9.1257(4)	37.191(3)
<i>c</i> (Å)	23.4789(14)	18.3195(8)	9.8276(7)
α (°)	90.00	90.00	90.00
β (°)	102.0240(10)	90.00	93.4270(10)
γ (°)	90.00	90.00	90.00
<i>V</i> (Å <sup>3</sup> )	4660.7(5)	2941.4(2)	3540.8(5)
<i>Z</i>	4	4	4
<i>D</i> <sub>calc</sub> (g/cm <sup>3</sup> )	1.812	1.549	1.578
<i>T</i> (K)	173(2)	173(2)	100(2)
μ(Mo Kα) (mm <sup>-1</sup> )	4.250	0.901	0.913
Unique data, <i>R</i> <sub>int</sub>	9761	3454	8222
Parameters/restraints	543/0	204/0	478/0
<i>R</i> <sub>1</sub> ( <i>I</i> > 2σ( <i>I</i> ))	0.0493	0.0418	0.0391
<i>R</i> <sub>1</sub> (all data)	0.0795	0.0493	0.0441
w <i>R</i> <sub>2</sub> (all data)	0.1168	0.1458	0.1032
	Hg <sub>2</sub> L <sub>1</sub> Cl <sub>4</sub> ( <b>6</b> )	HgL <sub>2</sub> <sub>2</sub> HgCl <sub>4</sub> ( <b>5</b> )	CuL <sub>2</sub> <sub>3</sub> (ClO <sub>4</sub> ) <sub>2</sub> ( <b>7</b> )
Chemical formula	C <sub>16</sub> H <sub>24</sub> C <sub>14</sub> Hg <sub>2</sub> N <sub>8</sub>	C <sub>20</sub> H <sub>32</sub> Cl <sub>4</sub> Hg <sub>2</sub> N <sub>8</sub>	C <sub>30</sub> H <sub>48</sub> Cl <sub>2</sub> CuN <sub>12</sub> O <sub>8</sub>
Molecular weight	871.41	927.52	839.24
Space group	<i>P</i> $\bar{1}$	<i>P</i> 2(1)/ <i>n</i>	<i>P</i> 2(1)/ <i>n</i>
Color	colorless	colorless	blue
<i>a</i> (Å)	8.6045(2)	16.995(3)	9.5258(11)
<i>b</i> (Å)	8.6444(2)	9.5747(14)	37.083(4)
<i>c</i> (Å)	8.8147(2)	17.531(3)	10.0098(12)
α (°)	108.4530(10)	90.00	90.00
β (°)	96.805(2)	113.641(2)	95.262(2)
γ (°)	109.4500(10)	90.00	90.00
<i>V</i> (Å <sup>3</sup> )	567.77(2)	2613.2(7)	3521.0(7)
<i>Z</i>	1	4	4
<i>D</i> <sub>calc</sub> (g/cm <sup>3</sup> )	2.549	2.358	1.583
<i>T</i> (K)	173(2)	100(2)	100(2)
μ(Mo Kα) (mm <sup>-1</sup> )	13.996	12.172	0.841
Unique data, <i>R</i> <sub>int</sub>	2671	5928	8205
Parameters/restraints	137/0	307/0	488/4
<i>R</i> <sub>1</sub> ( <i>I</i> > 2σ( <i>I</i> ))	0.0237	0.0292	0.0460
<i>R</i> <sub>1</sub> (all data)	0.0251	0.0331	0.0500
w <i>R</i> <sub>2</sub> (all data)	0.0549	0.0685	0.1212
	CuL <sub>2</sub> <sub>2</sub> (ClO <sub>4</sub> ) <sub>2</sub> ( <b>8</b> )	AgL <sub>2</sub> <sub>2</sub> BPh <sub>4</sub> ( <b>10</b> )	Ag <sub>2</sub> L <sub>1</sub> <sub>3</sub> (BPh <sub>4</sub> ) <sub>2</sub> ( <b>12</b> )
Chemical formula	C <sub>40</sub> H <sub>68</sub> Cl <sub>4</sub> Cu <sub>2</sub> N <sub>16</sub> O <sub>18</sub>	C <sub>44</sub> H <sub>52</sub> AgBN <sub>8</sub>	C <sub>72</sub> H <sub>76</sub> Ag <sub>2</sub> B <sub>2</sub> N <sub>12</sub>
Molecular weight	1329.98	811.62	1346.81
Space group	<i>P</i> 2(1)/ <i>n</i>	<i>P</i> $\bar{1}$	<i>P</i> $\bar{1}$
Color	blue	colorless	colorless
<i>a</i> (Å)	13.6639(15)	10.1692(16)	10.418(3)
<i>b</i> (Å)	8.7736(10)	11.3691(17)	21.453(6)
<i>c</i> (Å)	21.757(2)	17.836(3)	28.921(8)
α (°)	90.00	71.899(2)	108.846(4)
β (°)	94.121(2)	82.114(3)	91.832(5)
γ (°)	90.00	88.589(3)	95.322(5)
<i>V</i> (Å <sup>3</sup> )	2601.6(5)	1941.2(5)	6078(3)
<i>Z</i>	2	2	4
<i>D</i> <sub>calc</sub> (g/cm <sup>3</sup> )	1.698	1.389	1.472
<i>T</i> (K)	100(2)	100(2)	100(2)
μ(Mo Kα) (mm <sup>-1</sup> )	1.113	0.563	0.701
Unique data, <i>R</i> <sub>int</sub>	6031	8705	27084
Parameters/restraints	361/0	487/0	1585/0
<i>R</i> <sub>1</sub> ( <i>I</i> > 2σ( <i>I</i> ))	0.0377	0.0534	0.0471
<i>R</i> <sub>1</sub> (all data)	0.0439	0.0664	0.0664
w <i>R</i> <sub>2</sub> (all data)	0.1078	0.1296	0.1170

148.3; IR (KBr): 1602  $\text{cm}^{-1}$  ( $\text{N}=\text{C}=\text{N}$ ); Anal. Calc. for  $\text{Ag}(\text{C}_{10}\text{H}_{16}\text{N}_4)_2(\text{BC}_2\text{H}_2\text{O})[\text{Ag}(\text{BC}_2\text{H}_2\text{O})]_{0.9}$ : C, 65.88; H, 5.90; N, 9.37. Found: C, 65.59; H, 5.82; N, 9.14%.

#### 2.2.14. $[\text{Ag}_2(\mathbf{L1})_4](\text{BF}_4)_2$ , complex **11**

Addition of an amount of  $\text{AgBF}_4$  (156 mg, 0.800 mmol) to a solution of **L1** (268 mg, 1.63 mmol) in MeCN (20 mL) generated a light yellow solution. The reaction mixture was stirred overnight. After centrifugation, the MeCN supernatant was transferred to test tubes for recrystallization in the dark by ether diffusion. Colorless cubic crystals (308 mg, 74% yield) were harvested from the solution after several days.  $^1\text{H}$  NMR ( $\text{CD}_3\text{CN}$ , 399.75 MHz, ref. center line of  $\text{CD}_2\text{HCN}$  set at 1.96 ppm):  $\delta$  3.37 (s, 4H), 3.53–3.58 (t, 4H), 3.79–3.85 (t, 4H);  $^{13}\text{C}\{^1\text{H}\}$  NMR ( $\text{CD}_3\text{CN}$ , 100.52 MHz, ref.  $\text{CD}_3\text{CN}$  set at 117.6 ppm)  $\delta$  44.21, 51.98, 53.90, 156.19; IR (KBr): 1630  $\text{cm}^{-1}$  ( $\text{N}=\text{C}=\text{N}$ ); Anal. Calc. for  $\text{Ag}(\text{C}_8\text{H}_{12}\text{N}_4)_2\text{BF}_4$ : C, 36.74; H, 4.62; N, 21.42. Found: C, 36.58; H, 4.83; N, 21.16%.

#### 2.2.15. $[\text{Ag}_2(\mathbf{L1})_3](\text{BPh}_4)_2$ , complex **12**

Addition of an amount of  $\text{AgBF}_4$  (151 mg, 0.778 mmol) to a solution of **L1** (274 mg, 1.67 mmol) in MeCN (40 mL) yielded a colorless solution with a brown precipitate. After stirring for 6 h in the dark, one equivalent of  $\text{NaBPh}_4$  (267.0 mg, 0.780 mmol) was added to exchange the counteranion. Then the solution was stirred for 2 h in the dark. After filtering the insoluble brown solid off, the filtrate was concentrated to 20 mL. Then 100 mL of ethanol was added to produce a white precipitate. This white precipitate was collected and washed with additional EtOH, then dried under vacuum overnight to give a white solid (435 mg, 74% yield). Clear, colorless crystals were harvested after  $\text{Et}_2\text{O}$  diffusion into  $\text{CH}_3\text{CN}$  solution of this white solid in the dark over several days.  $^1\text{H}$  NMR ( $\text{CD}_3\text{CN}$ , 399.75 MHz, ref. center line of  $\text{CD}_2\text{HCN}$  set at 1.96 ppm):  $\delta$  3.38 (s,  $3 \times 4\text{H}$ ), 3.57 (t,  $3 \times 4\text{H}$ ), 3.84 (t,  $3 \times 4\text{H}$ ), 6.87 (t, 8H), 7.02 (t, 16H), 7.29 (m, 16H);  $^{13}\text{C}\{^1\text{H}\}$  NMR ( $\text{CD}_3\text{CN}$ , 100.52 MHz, ref.  $\text{CD}_3\text{CN}$  set at 117.6 ppm)  $\delta$  44.0, 51.8, 54.0, 122.1, 125.9, 136.0, 156.1; IR (KBr): 1621  $\text{cm}^{-1}$  ( $\text{N}=\text{C}=\text{N}$ ); Anal. Calc. for  $\text{Ag}_2(\text{C}_8\text{H}_{12}\text{N}_4)_3(\text{BC}_2\text{H}_2\text{O})_2$ : C, 64.21; H, 5.69; N, 12.48. Found: C, 64.21; H, 5.58; N, 12.50%.

### 2.3. X-ray crystallography

A summary of data collection and refinement results are presented in Table 1. Further details can be found in the CIF files deposited with CCDC. Software employed for structure determination include: APEX2 Version 2.2/SHELXTL (Bruker AXS Inc., 2007), AINT Version 7.34a (Bruker AXS Inc., 2007), SADABS Version 2007/2 (Sheldrick, Bruker AXS Inc.), XPREP Version 2005/2 (Sheldrick, Bruker AXS Inc.). The Bruker suite of programs APEX2/SHELXTL, SAINT, SADABS, XPREP may be obtained from Bruker AXS Inc., 5467 East Cheryl Parkway, Madison WI 53711. XS Version 2008/1 and XL Version 2008/1 [17].

X-ray crystal structure figures were prepared using Crystal-Maker 8.2 for Mac (CrystalMaker Software Ltd., Centre for Innovation and Enterprise, Oxford University Begbroke Science Park, Sandy Lane, Yarnton, Oxfordshire, OX5 1PF, UK; <http://www.crystalmaker.com>) Hydrogens, counterions and solvents have been removed for clarity. For all heavy atoms, 50% thermal ellipsoids are shown.

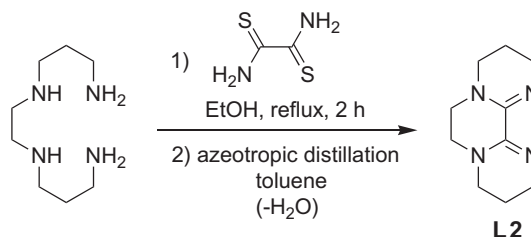
## 3. Results and discussion

### 3.1. Synthesis

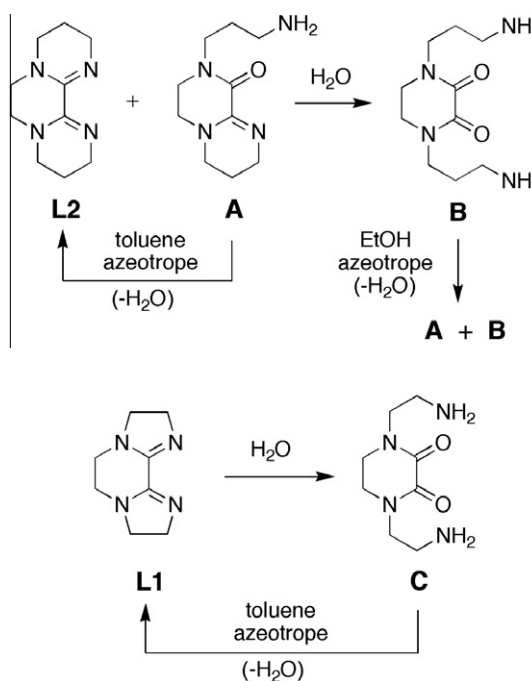
The bisamidine **L2** was prepared in a similar procedure as **L1** by the reaction of dithiooxamide and *N,N'*-bis-(3-aminopropyl)-1,2-

ethylenediamine (Scheme 1) [15]. In the case of **L2**, it was found that post-reaction azeotropic distillation with toluene was necessary in order to avoid contamination of the product by hydrolysis products (*vide infra*). The resulting solid had a yellow coloration due to traces of residual dithiooxamide. Although this was sufficiently pure for complexation studies by virtue of elemental and spectral analyses, it can be further purified by recrystallization from hexane or heptane followed by sublimation to give white crystalline **L2**.

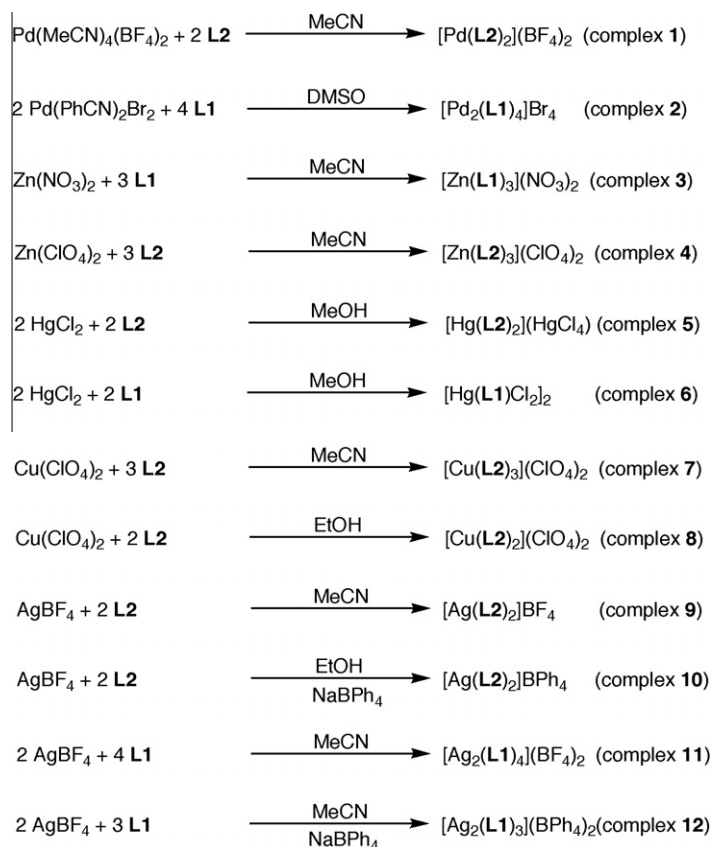
Our initial attempts to synthesize **L2** by the above dithiooxamide method were frustrated by the presence of an unexpected byproduct. NMR and mass spectra were consistent with contamination of **L2** by mixed amide–amidine **A** (Scheme 2), the result of apparent partial hydrolysis of **L2**. This hypothesis was confirmed by a series of NMR-scale experiments. When the **L2/A** mixture was dissolved in  $\text{D}_2\text{O}$ , proton and carbon NMR spectra showed the formation of fully hydrolyzed diamino-oxamide **B**. Attempted isolation of **B** by azeotropic removal of water with EtOH gave a mixture of **A** and **B**, showing that the hydrolysis is readily reversible (Scheme 2). With this observation in hand, the **L2/A** mixture was azeotropically distilled with toluene over a Dean-Stark trap, giving **L2** and thus leading to the modified procedure for the synthesis of **L2** noted above. The fact that this hydrolysis problem had to be overcome was a little surprising since no hydrolysis of **L1** had been observed in the past and no special precautions had been taken during its synthesis. As a control experiment, a small



Scheme 1. Synthesis of **L2**.



Scheme 2. Hydrolysis studies of **L1** and **L2**.



**Scheme 3.** Preparation of the metal complexes of **L1** and **L2**.

sample of **L1** was dissolved in D<sub>2</sub>O. In a matter of hours, **L1** was completely converted to diamino-oxamide **C** (NMR; kinetics have not been carried out). It was possible in this case to isolate the fully hydrolyzed product, **C**, and it was subsequently shown that it could be dehydrated back to **L1** using azeotropic distillation with toluene (Scheme 2). Qualitatively, **L2** is more sensitive towards hydrolysis than **L1**. While it is not clear whether this is a kinetic or a thermodynamic effect, both sequential hydrolyses appear to be completely reversible.

All described metal complexes were readily prepared in good yields by room-temperature reactions between **L1** and **L2** and the respective metal precursor in appropriate solvents such as acetonitrile, DMSO, methanol, or ethanol (Scheme 3). Resulting crude products were typically recrystallized by diethyl ether diffusion into a sample solution.

In contrast to the facile synthesis of the bimetallic cuprous [Cu<sub>2</sub>(**L1**)<sub>3</sub>](BF<sub>4</sub>)<sub>2</sub> complex from [Cu(CH<sub>3</sub>CN)<sub>4</sub>]<sub>2</sub>BF<sub>4</sub> [12], attempts to prepare Cu(I) complexes of **L2** were unsuccessful as the initially beige-colored solids were readily oxidized to Cu(II) products during purification procedures. The inability of **L2** to bridge cuprous centers and its stable chelation of Cu(II) likely contribute to this oxidation propensity.

### 3.2. Spectral characterization

A solid-state FT-IR spectrum of bisamidine **L1** displays strong symmetric and asymmetric N=C=C=N stretches at 1631 and 1616 cm<sup>-1</sup> respectively [13,14].

The solid-state FT-IR spectrum of new bisamidine ligand **L2** shows a broad and strong N=C=C=N band at 1601 cm<sup>-1</sup> and its electronic spectrum exhibits an intense π-π\* band at 248 nm (ε 7500 M<sup>-1</sup> cm<sup>-1</sup>). The proton NMR spectrum of ligand **L2** features two apparent triplets (N-CH<sub>2</sub>-CH<sub>2</sub>-CH<sub>2</sub>-N= : AA' and MM' of

AA'MM'XX' where the J<sub>AM</sub> type long-range couplings are small), one apparent pentet (N-CH<sub>2</sub>-CH<sub>2</sub>-CH<sub>2</sub>-N= : XX' of AA'MM'XX' where the J<sub>AM</sub> long-range couplings are small), and a singlet (N-CH<sub>2</sub>-CH<sub>2</sub>-N). Its <sup>13</sup>C{<sup>1</sup>H} NMR spectrum also suggests a C<sub>2v</sub> time-averaged geometry with only four upfield signals between δ 21.5 and 48.1 and the amidine resonance at δ 148.0.

All characterized complexes of **L1** and **L2** exhibit strong N=C=C=N stretches between 1525 and 1670 cm<sup>-1</sup> in their IR spectra. However, both symmetric and asymmetric stretches are clearly resolved in only two of these compounds.

#### 3.2.1. Palladium complexes **1** and **2**

A proton NMR spectrum of the [Pd(**L2**)<sub>2</sub>](BF<sub>4</sub>)<sub>2</sub> complex **1** in CD<sub>3</sub>CN suggests retention of the averaged bisamidine C<sub>2v</sub> symmetry albeit with downfield chemical shifts. The amidine <sup>13</sup>C{<sup>1</sup>H} NMR signal is also shifted downfield by 8.5 ppm from the free ligand value. Its monomeric nature in methanol solution was confirmed by an ESI-MS study which revealed a parent peak at 577.1 amu consistent with the [Pd(**L2**)<sub>2</sub>](BF<sub>4</sub>)<sup>+</sup> species. By contrast, the dimeric nature of complex **2**, [Pd<sub>2</sub>(**L1**)<sub>4</sub>]<sub>2</sub>Br<sub>4</sub>, in methanol was supported by its ESI-MS spectrum which featured a parent peak at 1106.5 amu for the [Pd<sub>2</sub>(**L1**)<sub>4</sub>]<sub>2</sub>Br<sub>3</sub><sup>+</sup> solution species. This is also in agreement with its solid-state (*vide infra*) structure which has approximate D<sub>4</sub> symmetry with an average twist angle of around 35° for the four bridging bisamidines. Interestingly, proton NMR spectra of the [Pd<sub>2</sub>(**L1**)<sub>4</sub>]<sub>2</sub>Br<sub>4</sub> complex **2** in either d<sub>6</sub>-DMSO or d<sub>4</sub>-methanol displayed only a singlet and two apparent triplets. This is indicative of an averaged bisamidine C<sub>2v</sub> symmetry due to a facile dynamic process. Although significant broadening of these signals was observed in d<sub>4</sub>-methanol, no decoalescence was observed down to -90 °C. Since no bisamidine exchange was found between free ligand and this complex, this fluxional process most likely in-

**Table 2**Selected bond data for the new metal complexes of **L1** and **L2**. For full structural details, see [Supplementary material](#).

Complex	Metal–N distance (Å)	Coordinated chelate amidine N–metal–N bite angle (°)	Coordinated amidine C=N (imino) distance (Å)	Coordinated amidine C–N (amino) distance (Å)	Coordinated amidine C–N (amino)–C angle sum (°)	Bisamidine N=C–C=N torsion angle (°)
Pd <sub>2</sub> <b>L1</b> <sub>4</sub> Br <sub>4</sub> ( <b>2</b> )	2.006(avg)		1.304(avg)	1.334(avg)	358.7(avg)	7.0–20.6
Zn <b>L1</b> <sub>3</sub> (NO <sub>3</sub> ) <sub>2</sub> ( <b>3</b> )	1.976 ( $\eta^1$ ) 2.079 ( $\eta^2$ )	83.53	1.295 1.287	1.337 1.335	357.6 355.2(avg)	3.6 4.8
Zn <b>L2</b> <sub>3</sub> (ClO <sub>4</sub> ) <sub>2</sub> ( <b>4</b> )	2.151(avg)	75.7(avg)	1.290(avg)	1.352(avg)	357.4(avg)	2.9–19.2
[Hg <b>L1</b> Cl <sub>2</sub> ] <sub>2</sub> ( <b>6</b> )	2.129 2.946		1.299 1.280	1.330 1.374	356.8 344.9	8.8
[Hg <b>L2</b> ] <sub>2</sub> HgCl <sub>4</sub> ( <b>5</b> )	2.251(avg)	73.4(avg)	1.294(avg)	1.340(avg)	358.2(avg)	–1.2–12.3
Cu <b>L2</b> <sub>3</sub> (ClO <sub>4</sub> ) <sub>2</sub> ( <b>7</b> )	2.324(ax) 2.027(eq)	73.3–79.4	1.290(avg)	1.351(avg)	358.2(avg)	5.6–20.9
Cu <b>L2</b> <sub>2</sub> (ClO <sub>4</sub> ) <sub>2</sub> ( <b>8</b> )	1.965(avg)	82.99(avg)	1.300(avg)	1.337(avg)	358.7(avg)	13.7(avg)
Ag <b>L2</b> <sub>2</sub> BPh <sub>4</sub> ( <b>10</b> )	2.299(avg)	71.5(avg)	1.288(avg)	1.357(avg)	357.9(avg)	8.7–20.9
Ag <sub>2</sub> <b>L1</b> <sub>3</sub> (BPh <sub>4</sub> ) <sub>2</sub> ( <b>12</b> )	2.104–2.209 ( $\mu^2$ ) 2.171–2.622 ( $\eta^2$ ) 2.095–2.109 2.725–2.820 (unsymmetrical- $\eta^2$ )	74.0	1.295(avg) 1.284(avg) 1.28(avg) 1.30(avg)	1.359(avg) 1.363(avg) 1.36(avg) 1.38(avg)	351.8(avg) 350.2(avg) 351(avg) 350(avg)	0.7 4.3 6.9(avg)

(avg) = average value; (ax) = axial; (eq) = equatorial; ( $\eta^1$ ) = monodentate; ( $\eta^2$ ) = chelating; ( $\mu^2$ ) = bimetallic bridging.

volves the intramolecular synchronized twisting of all bridging ligands about its Pd–Pd axis to attain an averaged  $D_{4h}$  symmetry.

### 3.2.2. Zinc complexes **3** and **4**

Since the solid-state structure of Zn(**L1**)<sub>3</sub>(NO<sub>3</sub>)<sub>2</sub>, **3**, features one chelating and two monodentate ligands while its proton and C-13 NMR spectra revealed a single set of ligand signals indicative of  $C_{2v}$  symmetry, a facile dynamic process must be occurring in solution to average all three bisamidines. Interestingly, complex **4** Zn(**L2**)<sub>3</sub>(ClO<sub>4</sub>)<sub>2</sub> displays two sets of unequal upfield bisamidine  $\beta$ -CH<sub>2</sub> multiplets (1.4:1 ratio) in its room-temperature proton NMR spectrum. Variable-temperature studies between –40 and +70 °C in CD<sub>3</sub>CN revealed a 1.3:1 ratio at –40° that increased with temperature till near coalescence at +70 °C (see [Supplementary material spectra 1 and 2](#)). One plausible explanation of this behavior may be the presence of a 2:1 as well as 3:1 complex in solution with the former increasingly favored by a higher temperature. Further studies are needed to confirm this hypothesis.

### 3.2.3. Mercury complexes **5** and **6**

The Hg(**L2**)<sub>2</sub>(HgCl<sub>4</sub>) complex **5** displayed solution spectral behavior consistent with a symmetrical bisamidine environment. Absence of <sup>13</sup>C–<sup>199</sup>Hg satellites in its C-13 NMR spectrum is consistent with facile ligand exchange. Although the X-ray structure of the dimeric complex **6**, [Hg(**L1**)Cl<sub>2</sub>]<sub>2</sub>, displayed an unsymmetrically-chelating ligand, its simple solution NMR spectra, again with absence of <sup>13</sup>C–<sup>199</sup>Hg satellites, indicated fast ligand exchange.

### 3.2.4. Silver complexes **9–12**

Like both the mercuric complexes, silver(I) complexes **9–12**; Ag(**L2**)<sub>2</sub>BF<sub>4</sub>, Ag(**L2**)<sub>2</sub>BPh<sub>4</sub>, Ag<sub>2</sub>(**L1**)<sub>4</sub>(BF<sub>4</sub>)<sub>2</sub>, and Ag<sub>2</sub>(**L1**)<sub>3</sub>(BPh<sub>4</sub>)<sub>2</sub> all display a single set of bisamidine proton signals indicative of averaged  $C_{2v}$  ligand geometry and facile exchange with any added free ligand. Consistent with this rapid exchange, no <sup>13</sup>C–<sup>107,109</sup>Ag satellites were observed. As described in the next section, in the solid-state complexes **10** and **12**, Ag(**L2**)<sub>2</sub>BPh<sub>4</sub> and Ag<sub>2</sub>(**L1**)<sub>3</sub>(BPh<sub>4</sub>)<sub>2</sub>, were found to have very different coordination modes.

## 3.3. X-ray structural studies

Crystal structure data for the nine new complexes are summarized in [Table 1](#). Relevant bond lengths and angles are collected in

[Table 2](#). Full details of the structural determinations and bond data can be found in the [Supplementary material](#).

While both **L1** and **L2** are prestrained so as to present a limited range of synperiplanar N=C–C=N torsion angles centered about zero ([Table 2](#)), new ligand **L2** is more conformationally flexible because of the distal six-membered rings. Two basic types of conformations are observed in the chelated **L2** ligands of the structures reported herein. In one type, the central methylene of each –CH<sub>2</sub>–CH<sub>2</sub>–CH<sub>2</sub>– distal ring “flap” is distorted in the same direction away from the mean plane of the bisamidine unit of the ligand (denoted *SYN* for the purpose of further discussion). Symmetry is  $C_1$  rather than  $C_s$  in this case. In the second type, the two flaps are distorted in opposite directions relative to the mean plane (denoted *ANTI*) and the ligand has approximate  $C_2$  symmetry. There is no apparent correlation between the type of conformation and the magnitude of the observed N=C–C=N torsion angles in the coordination complexes. Both *SYN* and *ANTI* are observed to have torsion angles ranging up to approximately 20°. In one case (*vide infra*), disorder between these two conformational types is observed. It is likely that the energy difference between such conformations is small, and possible that the preference is determined by packing.

### 3.3.1. The [Pd<sub>2</sub>(**L1**)<sub>4</sub>]Br<sub>4</sub> complex **2**

In this dimeric structure approximating  $D_4$  symmetry, the two palladium centers are held at a distance of 2.741(6) Å by four bridging bisamidines which exhibit a twist angle of about 35° down the Pd–Pd axis ([Fig. 2](#)). All Pd–N distances are very similar, ranging only from 1.998 to 2.014 Å. An essentially square-planar PdN<sub>4</sub> coordination sphere is found around each metal center. The lengthened average C=N bond length of 1.30 Å (compared to the uncoordinated diimino C=N distance of 1.27–1.28 Å, *vide infra*) is consistent with strong Pd–N bonding due to amidine conjugation. The diimine (N=C–C=N) dihedral angles are splayed out from 7° to 21° to accommodate metal bridging. A dipalladium complex bridged by two bioxazolines has been structurally characterized and here the Pd–Pd separation was found to be substantially longer at 2.894 Å [[18](#)]. A formamidinate-bridged palladium(II) dimer of  $D_4$  symmetry has been reported in the literature [[19](#)]. Its Pd–Pd separation is substantially shorter at 2.555(1) Å due to its smaller NCN bridging units.

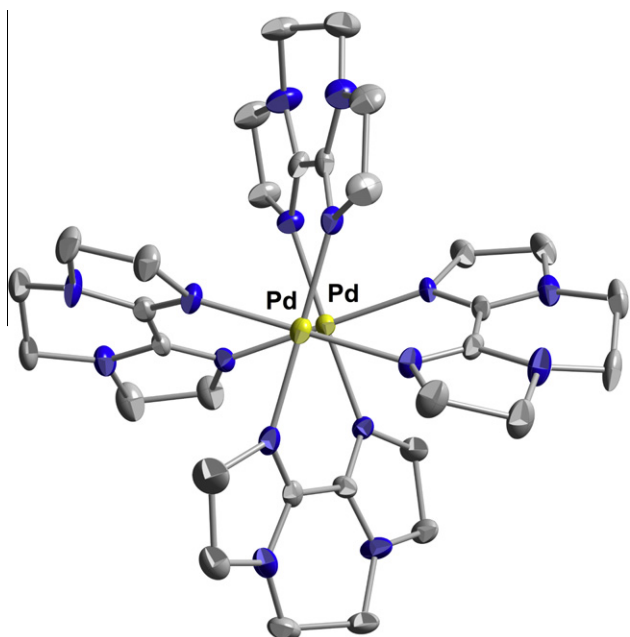


Fig. 2. Structure of  $[\text{Pd}_2(\text{L}1)_4]\text{Br}_4$ , complex 2. Bromides not shown.

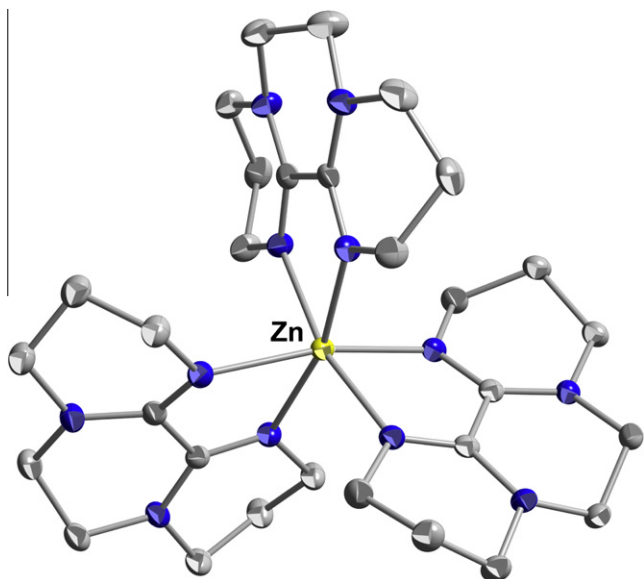


Fig. 3. Structure of  $\text{Zn}(\text{L}2)_3(\text{ClO}_4)_2$ , complex 4. Perchlorates not shown.

### 3.3.2. The $\text{Zn}(\text{L}1)_3(\text{NO}_3)_2$ and $\text{Zn}(\text{L}2)_3(\text{ClO}_4)_2$ complexes 3 and 4

The six-coordinate complex 4,  $\text{Zn}(\text{L}2)_3(\text{ClO}_4)_2$ , structure approximates overall  $D_3$  symmetry with a trigonal twist angle of  $45^\circ$  (Fig. 3). An average Zn–N distance of 2.15 Å and bite angle of  $75.7^\circ$  are close to the idealized  $\text{L}2$  metal chelation geometry. The ligand is not severely-distorted from planarity as indicated by an average amino C–N–C angle sum of  $357^\circ$ . An average C=N distance of 1.29 Å and C–N of 1.35 Å are observed. All three of the  $\text{L}2$  ligands in the complex adopt *SYN* conformations with N=C–C=N torsion angles of the same sign ranging from  $2.9^\circ$  to  $19.2^\circ$ . Three structural reports of Zn(II) complexes with three chelating biimidazoles or bioxazolines have appeared [20–22]. All these have very similar N–Zn–N bite angles of  $76$ – $79^\circ$ , Zn–N distances of 2.16–2.26 Å, C=N bond lengths of 1.26–1.33 Å, and N=C–C=N torsion angles of  $0.5$ – $8.8^\circ$ .

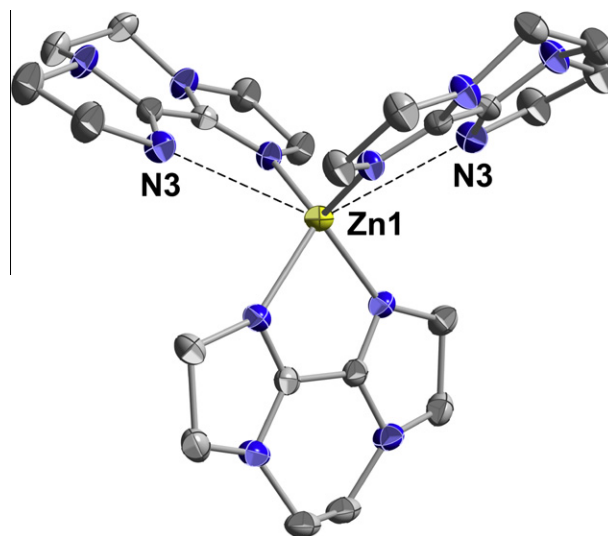


Fig. 4. Structure of  $\text{Zn}(\text{L}1)_3(\text{NO}_3)_2$ , complex 3. Nitrates omitted.

By contrast, only one bisamidine in complex 3,  $\text{Zn}(\text{L}1)_3(\text{NO}_3)_2$ , is chelating while the remaining two are essentially monodentate (Zn(1)···N(3) separation is over 3.00 Å), yielding a *pseudo*-tetrahedral Zn(II) coordination sphere (Fig. 4). A  $C_2$  axis passes through the metal and chelating ligand with N–Zn–N bite angle of  $83.5(1)^\circ$ , far from the idealized  $35^\circ$  for the free ligand. The chelating Zn–N distance of 1.976(2) Å is significantly longer than the monodentate Zn–N distance of 2.079(2) Å. Within the monodentate  $\text{L}1$ , the coordinated C=N is elongated to 1.295(3) Å compared to 1.276(3) Å for the uncoordinated C=N bond, while the N–C bond is significantly shorter (1.337(3) Å) upon coordination compared to the uncoordinated side (1.379(3) Å). The sum of C–N–C bond angles around the bound amidine ring amino nitrogen N(2) ( $357.6(3)^\circ$ ) is close to planarity compared to a much more pyramidalized N(4) ( $344.7(3)^\circ$ ) in the uncoordinated amidine. These data are fully consistent with associated amidine polarization upon metal coordination.

### 3.3.3. The $[\text{Hg}(\text{L}2)_2]\text{HgCl}_4$ and $[\text{Hg}(\text{L}1)\text{Cl}_2]_2$ complexes 5 and 6

The structure of the  $[\text{Hg}(\text{L}1)\text{Cl}_2]_2$  complex 6 has inversion symmetry with two bridging chlorides, one terminal chloride, and an unsymmetrically-chelating bisamidine at each five-coordinate mercuric center (Fig. 5). The two disparate Hg–N bond-lengths are 2.129(4) and 2.946(4) Å. As a result, the strongly-bound amidine C=N is slightly lengthened to 1.299(5) Å compared to 1.280(6) Å for the weakly-bound C=N group, while the amidine C–N bond shortens significantly to 1.330(5) Å from 1.374(5) Å. Consistent with increased amidine polarization, this amino N's C–N–C angles sum to a near-planar  $356.7(6)^\circ$ .

The complex 5,  $[\text{Hg}(\text{L}2)_2]\text{HgCl}_4$ , structure features a mercury coordination geometry that approximates a trigonal bipyramid

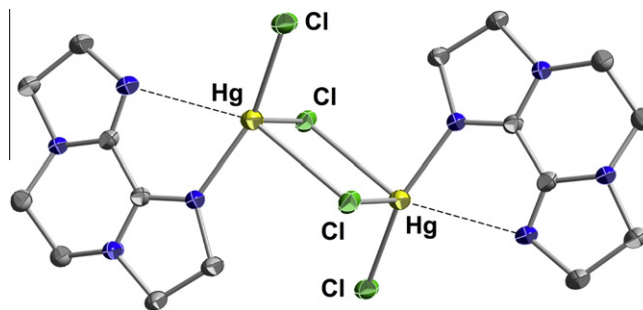


Fig. 5. Structure of  $[\text{Hg}(\text{L}1)\text{Cl}_2]_2$ , complex 6.

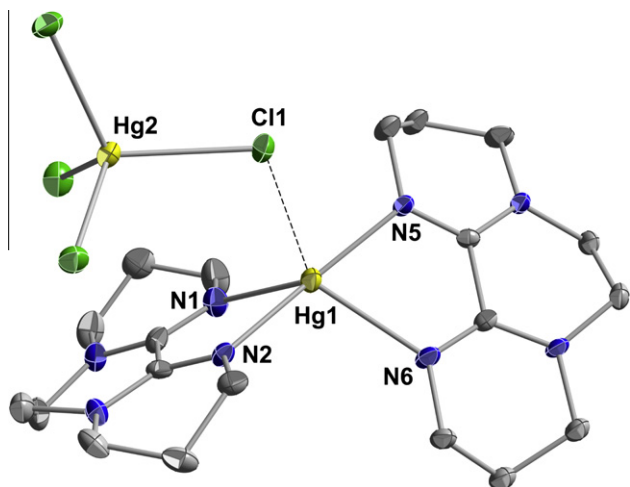


Fig. 6. Structure of  $[\text{Hg}(\text{L}2)_2]\text{HgCl}_4$ , complex 5.

( $\tau = 0.825$ ) [23] with one weak equatorial coordination of the  $\text{HgCl}_4^{2-}$  dianion through a Cl bridge at 3.045(5) Å (Fig. 6). The axial N(2)–Hg(1)–N(5) angle is 170.3(2)° while equatorial N(1)–Hg(1)–N(6) angle is 120.8(2)°. The chelating bisamidines have bite angles of 73°, close to the idealized value of 75° for **L2**. Hg–N bond distances within the chelate ring, however, are somewhat unsymmetrical with Hg(1)–N(1) significantly longer at 2.329(5) Å compared to Hg(1)–N(2) at 2.151(4) Å, for example. The average C–N–C angle sum at the amino N's is 358.3°. The ligand with the  $\text{HgCl}_4$  moiety perched above is *ANTI* with a N=C–C=N torsion angle of  $-1.2^\circ$ , while the other is *SYN* with a 12.3° torsion angle.

### 3.3.4. The $\text{Cu}(\text{L}2)_3(\text{ClO}_4)_2$ and $\text{Cu}(\text{L}2)_2(\text{ClO}_4)_2$ complexes 7 and 8

The 3:1 complex **7**  $\text{Cu}(\text{L}2)_3(\text{ClO}_4)_2$  has a similar structure to the previously-reported  $\text{Cu}(\text{L}1)_3(\text{ClO}_4)_2$  featuring a tetragonal geometry with Jahn–Teller elongations along the N(5)–Cu(1)–N(12) axis (Fig. 7). One symmetrically and two unsymmetrically-chelating bisamidines are found in each case, though the weaker axial Cu–N bonds are substantially elongated in  $\text{Cu}(\text{L}1)_3(\text{ClO}_4)_2$  at 2.81 and

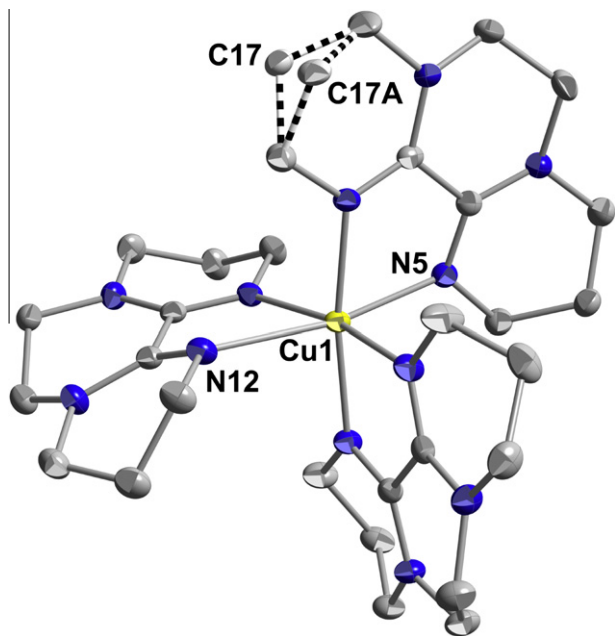


Fig. 7. Structure of  $\text{Cu}(\text{L}2)_3(\text{ClO}_4)_2$ , complex 7. Perchlorates omitted.

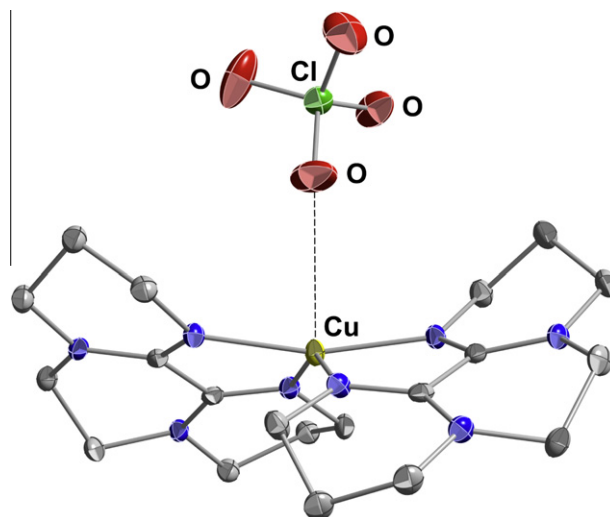


Fig. 8. Structure of  $\text{Cu}(\text{L}2)_2(\text{ClO}_4)_2$ , complex 8. Only one perchlorate shown.

2.84 Å, likely due to its smaller idealized bite angle. One of the unsymmetrically-chelating **L2** ligands adopts the *SYN* conformation with a relatively large N=C–C=N torsion angle of 20.1°. The other exhibits two-site torsional disorder in one of the distal six-rings (*SYN* and *ANTI*, indicated by the two half-occupancy carbons C(17)/C(17a) connected through two-tone bonds). The symmetrically chelating **L2** adopts a *SYN* conformation with a N=C–C=N torsion angle of  $-5.6^\circ$ .

The monomeric 2:1 complex **8**,  $\text{Cu}(\text{L}2)_2(\text{ClO}_4)_2$ , features a very distorted square pyramidal Cu(II) ( $\tau = 0.27$ ) with two chelating equatorial ligands and a weak axial perchlorate coordination at 2.817 Å (Fig. 8). Strong Cu–N bonding is indicated by the short average distance of 1.965 Å, lengthened C=N of 1.300 Å and shortened amino-C of 1.337 Å. One of the ligands adopts the *SYN* and the other the *ANTI* conformation, with similar N=C–C=N torsion angles of 12.1° and 15.2° respectively. This structure contrasts dramatically with the reported dimeric structure of  $[\text{Cu}(\text{L}1)_2]_2(\text{ClO}_4)_4$  which has a Cu–Cu distance of 2.775(1) Å supported by four bridging bisamidines [12].

### 3.3.5. The $\text{Ag}(\text{L}2)_2\text{BPh}_4$ and $\text{Ag}_2(\text{L}1)_3(\text{BPh}_4)_2$ complexes 10 and 12

A severely-distorted tetrahedral silver coordination is revealed in the structure of complex **10**,  $\text{Ag}(\text{L}2)_2\text{BPh}_4$ , with two chelating bisamidines with N–Ag–N bite angles nearing 72° (Fig. 9). Each li-

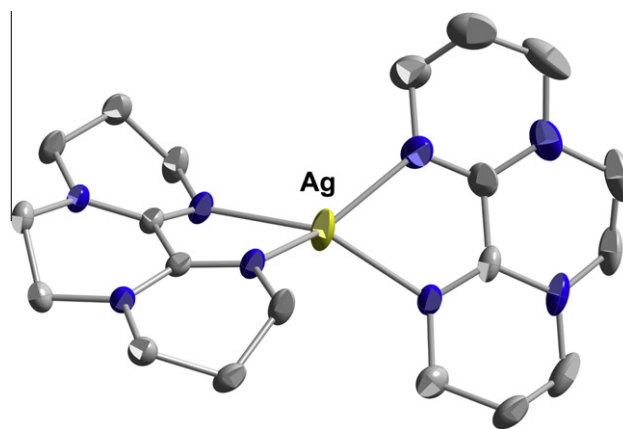


Fig. 9. Structure of  $\text{Ag}(\text{L}2)_2\text{BPh}_4$ , complex 10. Anion omitted.

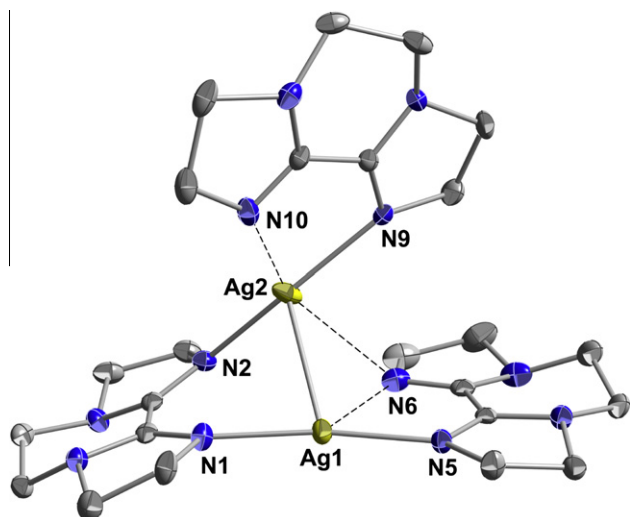


Fig. 10. Structure of  $\text{Ag}_2(\text{L1})_3(\text{BPh}_4)_2$ , complex **12**. Anions not shown.

gand is flattened with an amine bond angle sum of  $358^\circ$ . The two ligands are conformationally distinct in the complex, one having the *SYN* and the other the *ANTI* conformation, with  $\text{N}=\text{C}-\text{C}=\text{N}$  torsion angles of  $-8.7^\circ$  and  $20.9^\circ$  respectively.

By contrast, the two independent  $\text{Ag}_2(\text{L1})_3(\text{BPh}_4)_2$  dimeric units in the X-ray structure of complex **12** both feature three distinct **L1** coordination modes: symmetrical bridging, unsymmetrical chelating, as well as unsymmetrical bridging (Fig. 10).

Only one of these units will be discussed. The  $\text{Ag}(1)-\text{Ag}(2)$  distance of  $2.8749(6)$  Å is shorter than that found in metallic silver ( $2.89$  Å) and considerably shorter than their van der Waals sum of  $3.44$  Å. BIIM-bridged as well as unbridged  $\text{Ag}_2$  structures have been reported [20]. Silver–silver separations of  $2.83$ – $3.08$  Å are observed. Here in  $\text{Ag}_2(\text{L1})_3(\text{BPh}_4)_2$ ,  $\text{Ag}(2)$  is five-coordinate while  $\text{Ag}(1)$  has a T-shaped coordination sphere augmented by a weak interaction with a bridging amidine nitrogen ( $\text{N}(6)$ ). As a result, disparate  $\text{Ag}-\text{N}$  bond lengths are observed; symmetrical bridging  $\text{Ag}-\text{N}$  distances range from  $2.104(3)$  to  $2.209(3)$  Å, and unsymmetrical bridging is indicated by  $\text{Ag}(1)-\text{N}(5)$  at  $2.095(3)$  Å and  $\text{Ag}(2)-\text{N}(6)$  at  $2.820(3)$  Å. However, the approach angle for  $\text{N}(6)$  to  $\text{Ag}(2)$  is far from ideal. In fact, this nitrogen is better oriented for a very long chelation to  $\text{Ag}(1)$  at a  $3.086$  Å distance. Less exaggerated unsymmetrical chelation is seen in the pair of  $\text{Ag}(2)-\text{N}(9)$  and  $\text{Ag}(2)-\text{N}(10)$  bond lengths of  $2.244(3)$  and  $2.551(3)$  Å.

#### 4. Summary and conclusions

With the characterization of these eleven new complexes including nine X-ray structural studies, the tricyclic bisamidines **L1** and **L2** have been shown to have extensive metal coordination chemistry. To date **L1**, with divergent donor lone pairs, has been found in monodentate, symmetrical and unsymmetrical chelating, as well as symmetrical and unsymmetrical metal-bridging modes in its solid-state structures. These include  $\text{Mn}(\text{II})$ ,  $\text{Fe}(\text{II})$ ,  $\text{Ru}(\text{II})$ ,

$\text{Co}(\text{II})$ ,  $\text{Pd}(\text{II})$ ,  $\text{Cu}(\text{I})$ ,  $\text{Cu}(\text{II})$ ,  $\text{Ag}(\text{I})$ ,  $\text{Zn}(\text{II})$ ,  $\text{Cd}(\text{II})$ ,  $\text{Hg}(\text{II})$ , as well as several lanthanide(III) complexes (La, Eu, Gd, and Lu) [24]. The design of **L2** with two six-membered bisamidinate rings in its backbone to provide significantly more convergent lone pairs was intended to favor the chelation mode. Indeed, this has been the only experimentally-observed coordination mode in X-ray structures of its  $\text{Cu}(\text{II})$ ,  $\text{Zn}(\text{II})$ ,  $\text{Hg}(\text{II})$ ,  $\text{Ag}(\text{I})$ ,  $\text{Eu}(\text{III})$  and  $\text{Gd}(\text{III})$  complexes [14]. These data confirm our premise that tuning of the coordination chemistry of this family of tricyclic bisamidines can be readily attained through ring size variations. Finally, in all complexes studied, coordination of the amidine moiety results in lengthening of its  $\text{C}=\text{N}$  bond, shortening of its  $\text{C}-\text{N}$  bond, and a less pyramidal amine nitrogen, entirely consistent with anticipated coordination-induced polarization of the amidine unit.

#### Appendix A. Supplementary material

CCDC 777814, 777815, 777816, 777817, 777818, 777819, 777820, 777821 and 777822 contains the supplementary crystallographic data for this paper. These data can be obtained free of charge from The Cambridge Crystallographic Data Centre via [http://www.ccdc.cam.ac.uk/data\\_request/cif](http://www.ccdc.cam.ac.uk/data_request/cif). Supplementary data associated with this article can be found, in the online version, at [doi:10.1016/j.ica.2010.08.015](https://doi.org/10.1016/j.ica.2010.08.015).

#### References

- [1] A.P. Smith, C.L. Fraser, *Compr. Coord. Chem. II* 1 (2004) 1.
- [2] B.-H. Ye, M.-L. Tong, X.-M. Chen, *Coord. Chem. Rev.* 249 (2005) 545.
- [3] O. Maury, H. Le Bozec, *Acc. Chem. Res.* 38 (2005) 691.
- [4] V. Balzani, G. Bergamini, F. Marchioni, P. Ceroni, *Coord. Chem. Rev.* 250 (2006) 1254.
- [5] C.R. Luman, F.N. Castellano, *Compr. Coord. Chem. II* 1 (2004) 25.
- [6] R.D. Hancock, D.L. Melton, J.M. Harrington, F.C. McDonald, R.T. Gephart, L.L. Boone, S.B. Jones, N.E. Dean, J.R. Whitehead, G.M. Cockrell, *Coord. Chem. Rev.* 251 (2007) 1678.
- [7] M. Tadokoro, K. Nakasuji, *Coord. Chem. Rev.* 198 (2000) 205.
- [8] J.C. Yoder, J.P. Roth, E.M. Gussenhoven, A.S. Larsen, J.M. Mayer, *J. Am. Chem. Soc.* 125 (2003) 2629.
- [9] D. Rechavi, M. Lemaire, *Chem. Rev. (Washington, DC, US)* 102 (2002) 3467.
- [10] S. Dagonne, S. Bellemin-Lapponnaz, A. Maisee-Francois, *Eur. J. Inorg. Chem.* (2007) 913.
- [11] A. Pfaltz, *Asymmetric Synth.* (2007) 131.
- [12] D.W. Widlicka, E.H. Wong, G.R. Weisman, K.C. Lam, R.D. Sommer, C.D. Incarvito, A.L. Rheingold, *Inorg. Chem. Commun.* 3 (2000) 648.
- [13] D.W. Widlicka, MS Thesis, Department of Chemistry, University of New Hampshire, Durham, NH, USA, 2002.
- [14] J. Li, MS Thesis, Department of Chemistry, University of New Hampshire, Durham, NH, USA, 2007.
- [15] D.P. Reed, G.R. Weisman, *Org. Synth.* 78 (2002) 73.
- [16] I. Saikawa, T. Hori, K. Momoi, Y. Kobane, T. Yasuda, M. Miyahara, S. Tai, H. Tsuda, M. Doi, S. Kishimoto, in: Toyama Chemical Co., Ltd., Japan, Patent Application: JP, 1979, p. 10.
- [17] G.M. Sheldrick, *Acta Crystallogr., Sect. A* A64 (2008) 112.
- [18] A. Scarel, J. Durand, D. Franchi, E. Zangrando, G. Mestroni, C. Carfagna, L. Mosca, R. Seraglia, G. Consiglio, B. Milani, *Chem.-Eur. J.* 11 (2005) 6014.
- [19] F.A. Cotton, J. Gu, C.A. Murillo, D.J. Timmons, *J. Am. Chem. Soc.* 120 (1998) 13280.
- [20] R.-L. Sang, L. Xu, *Eur. J. Inorg. Chem.* (2006) 1260.
- [21] R.Q. Zou, Q. Xu, *Acta Crystallogr., Sect. E: Struct. Rep.* E61 (2005) m1075.
- [22] G.K. Patra, I. Goldberg, A. Sarkar, S. Chowdhury, D. Datta, *Inorg. Chim. Acta* 344 (2003) 7.
- [23] A.W. Addison, T.N. Rao, J. Reedijk, J. Van Rijn, G.C. Verschoor, *J. Chem. Soc., Dalton Trans.* (1984) 1349.
- [24] K.A. Fichter, MS Thesis, Department of Chemistry, University of New Hampshire, Durham, NH, USA, 2004.